*Inorg. Chem.* **2006**, *45*, 8799–8806


# Mononitrosyl Tris(Thiolate) Iron Complex $[Fe(NO)(SPh)_3]^-$ and Dinitrosyl Iron Complex $[(EtS)_2Fe(NO)_2]^-$: Formation Pathway of Dinitrosyl Iron Complexes (DNICs) from Nitrosylation of Biomimetic Rubredoxin $[Fe(SR)_4]^{2-/1-}$ (R = Ph, Et)

**Tsai-Te Lu, Show-Jen Chiou, Chun-Yu Chen, and Wen-Feng Liaw***

*Department of Chemistry, National Tsing Hua University, Hsinchu 30013, Taiwan*

Received August 1, 2006

Nitrosylation of the biomimetic reduced- and oxidized-form rubredoxin $[Fe(SR)_4]^{2-/1-}$ (R = Ph, Et) in a 1:1 stoichiometry led to the formation of the extremely air- and light-sensitive mononitrosyl tris(thiolate) iron complexes (MNICs) $[Fe(NO)(SR)_3]^-$ along with byproducts $[SR]^-$ or $(RS)_2$. Transformation of $[Fe(NO)(SR)_3]^-$ into dinitrosyl iron complexes (DNICs) $[(RS)_2Fe(NO)_2]^-$ and Roussin's red ester $[Fe_2(\mu\text{-}SR)_2(NO)_4]$ occurs rapidly under addition of 1 equiv of $NO_{(g)}$ and $[NO]^+$, respectively. Obviously, the mononitrosyl tris(thiolate) complex $[Fe(NO)(SR)_3]^-$ acts as an intermediate when the biomimetic oxidized- and reduced-form rubredoxin $[Fe(SR)_4]^{2-/1-}$ exposed to $NO_{(g)}$ were modified to form dinitrosyl iron complexes $[(RS)_2Fe(NO)_2]^-$. Presumably, NO binding to the electron-deficient $[Fe^{III}(SR)_4]^-$ and $[Fe^{III}(NO)(SR)_3]^-$ complexes triggers reductive elimination of dialkyl/diphenyl disulfide, while binding of NO radical to the reduced-form $[Fe^{II}(SR)_4]^{2-}$ induces the thiolate-ligand elimination. Protonation of $[Fe(NO)(SEt)_3]^-$ yielding $[Fe(NO)(SPh)_3]^-$ by adding 3 equiv of thiophenol and transformation of $[Fe(NO)(SPh)_3]^-$ to $[Fe(NO)(SEt)_3]^-$ in the presence of 3 equiv of $[SEt]^-$, respectively, demonstrated that complexes $[Fe(NO)(SPh)_3]^-$ and $[Fe(NO)(SEt)_3]^-$ are chemically interconvertible. Mononitrosyl tris(thiolate) iron complex $[Fe(NO)(SPh)_3]^-$ and dinitrosyl iron complex $[(EtS)_2Fe(NO)_2]^-$ were isolated and characterized by X-ray diffraction. The mean NO bond distances of 1.181(7) Å (or 1.191(7) Å) in complex $[(EtS)_2Fe(NO)_2]^-$ are nearly at the upper end of the 1.178(3)–1.160(6) Å for the anionic $\{Fe(NO)_2\}^9$ DNICs, while the mean FeN(O) distances of 1.674(6) Å (or 1.679(6) Å) exactly fall in the range of 1.695(3)–1.661(4) Å for the anionic $\{Fe(NO)_2\}^9$ DNICs.

## Introduction

Dinitrosyl iron complexes (DNICs) have been suggested as intermediates of iron-catalyzed degradation and formation of S-nitrosothiols (RSNO) and as one of two possible forms for storage and transport of NO in biological systems.[1] Extensive EPR studies have identified nitrosyl non-heme iron complexes as products from the interaction of NO with several iron−sulfur and other iron-containing proteins.[1−5] Coordination of NO with [Fe−S] clusters is thought to result in impairment of metabolic functions.[6] It is also proposed

* To whom correspondence should be addressed. E-mail: wfliaw@mx.nthu.edu.tw.

(1) (a) Stamler, J. S. *Cell* **1994**, *78*, 931−936. (b) Stamler, J. S.; Singel, D. J.; Loscalzo, J. *Science* **1992**, *258*, 1898−1902. (c) Ford, P. C.; Lorkovic, I. M. *Chem. Rev.* **2002**, *102*, 993−1017. (d) Butler, A. R.; Megson, I. L. *Chem. Rev.* **2002** *102*, 1155−1166. (e) Ueno, T.; Susuki, Y.; Fujii, S.; Vanin, A. F.; Yoshimura, T. *Biochem. Pharmacol.* **2002**, *63*, 485−493. (f) Frederik. A. C.; Wiegant, I. Y.; Malyshev, I. Y.; Kleschyov, A. L.; van Faassen, E.; Vanin, A. F. *FEBS Lett* **1999**, *455*, 179−182. (g) Lee, J.; Chen, L.; West, A. H.; Richter-Addo, G. B. *Chem. Rev.* **2002**, *102*, 1019−1065. (h) McCleverty, J. A. *Chem. Rev.* **2004**, *104*, 403−418. (i) Hayton, T. W.; Legzdins, P.; Sharp, W. B. *Chem. Rev.* **2002**, *102*, 935−991. (j) Wang, P. G.; Xian, M.; Tang, X.; Wu, X.; Wen, Z.; Cai, T.; Janczuk, A. J. *Chem. Rev.* **2002**, *102*, 1091−1134.

(2) (a) Badorff, C.; Fichtlscherer, B.; Muelsch, A.; Zeiher, A. M.; Dimmeler, S. *Nitric Oxide* **2002**, *6*, 305−312. (b) Mulsch, A.; Mordvintcev, P. I.; Vanin, A. F.; Busse, R. *FEBS Lett.* **1991**, *294*, 252−256.

(3) (a) Cruz-Ramos, H.; Crack, J.; Wu, G,; Hughes, M. N.; Scott, C.; Thomson, A. J.; Green, J.; Poole, R. K. *EMBO J.* **2002,** *21*, 3235−3244. (b) Sellers, V. M.; Johnson, M. K.; Dailey, H. A. *Biochemistry* **1996**, *35*, 2699−2704. (c) Schmidt, H. H. H. W *FEBS Lett.* **1992**, *307*, 102−107.

(4) Cesareo, E.; Parker, L. J.; Pedersen, J. Z.; Nuccetelli, M.; Mazzetti, A. P.; Pastore, A.; Federici, G.; Caccuri, A. M.; Ricci, G.; Adams, J. J.; Parker, M. W.; Bello, M. L. *J. Biol. Chem.* **2005**, *280*, 42172−42180.

(5) (a) Foster, M. W.; Cowan, J. A. *J. Am. Chem. Soc.* **1999**, *121*, 4093−4100. (b) Lancaster, J. R., Jr.; Hibbs. J. B., Jr. *Proc. Natl. Acad. Sci. U.S.A.* **1990**, *87*, 1223−1227.

10.1021/ic061439g CCC: $33.50 
Published on Web 09/01/2006

that the interplay between NO (or some NO-derived molecules) and [Fe−S] clusters at critical catalytic sites is crucial in the response to environmental signals within cells.[6] In addition, nitrite was demonstrated as a highly effective species in inducing posttranslational modifications normally associated with NO, such as heme nitrosylation and S-nitrosation, in a variety of mammalian tissues.[7] Examples of nitric oxide coordination to iron and the spectroscopic signals of dinitrosyl iron complexes are of much interest, particularly in light of role(s) in sulfur-rich protein uptake and degradation.[1−7] Recently, EPR and UV−vis absorption studies demonstrated that mammalian ferrochelatase is strongly inhibited by nitric oxide via degradation of the [2Fe−2S] clusters to form cysteinyl-coordinated monomeric iron−dinitrosyl complex.[8] In addition, activation of SoxR protein, a redox-sensitive transcription activator, in *Escherichia coli* on exposure to macrophage-generated NO was suggested to occur through nitrosylation of the [2Fe−2S] clusters to form protein-bound dinitrosyl−iron dithiol adducts.[9] In particular, Ding and co-workers showed that when *E. coli* cells are exposed to nitric oxide, the ferredoxin [2Fe−2S] clusters are modified to form protein-bound dinitrosyl iron complexes. In the repair of the nitric oxide-modified ferredoxin [2Fe−2S] cluster, the dinitrosyl iron complexes can be directly transformed back to the ferredoxin [2Fe−2S] cluster by cysteine desulfurase (IscS) and L-cysteine in vitro with no need for the addition of iron or any other protein components.[10]

As has been known, characterization of both protein-bound and low-molecular-weight DNICs in vitro has been made possible via their distinctive EPR signals at $g = 2.03$.[1−10] To our knowledge, also known in inorganic chemistry is the precedence for small-molecule DNICs in four oxidation levels of the $\{Fe(NO)_2\}$ unit, including the EPR-active (i) anionic $\{Fe(NO)_2\}$,[9] (ii) neutral $\{Fe(NO)_2\}$,[9] and (iii) cationic $\{Fe(NO)_2\}$[9] DNICs coordinated by $[SR]^-$ and N-containing ligands, as well as (iv) the EPR-silent, neutral $\{Fe(NO)_2\}$[10] DNICs coordinated by CO, $PPh_3$, and N-containing ligands.[11−13] Here the electronic structure/state of $M(NO)_2$ unit of DNICs is generally designated as $\{M(NO)_2\}^n$ (M = transition metal). This formalism $\{M(NO)_2\}^n$ invokes the Enemark−Feltham notation which stresses the well-known covalence and delocalization in the electronically amorphous $M(NO)_2$ unit.[14]

In model compounds, a study with synthetic models proposed that [2Fe−2S], as well as [4Fe−4S], clusters reacting with NO, respectively, yield DNICs which can give rise to the EPR $g = 2.03$ signal.[1d] Very recently, Lippard and co-workers reported that reaction of $[Fe(S^tBu)_4]^{2-}$ and $NO_{(g)}$ in $CH_3CN$−THF led to the formation of $[Fe(NO)(S^tBu)_3]^-$,[15a] and the electronic structure of $[Fe(NO)(S^tBu)_3]^-$ was characterized as $[Fe^{III}(NO^-)(S^tBu)_3]^-$.[15] The mononitrosyl iron tris(thiolate) complex (MNIC) $[Fe(NO)(S^tBu)_3]^-$ was subsequently converted into $[(S^tBu)_2Fe(NO)_2]^-$ under limited $NO_{(g)}$.[15a] We have shown that nitrosylation of the [2Fe−2S] cluster $[S_5Fe(\mu\text{-}S)_2FeS_5]^{2-}$ yielding $[S_5Fe(NO)_2]^-$, and the reversible transformation of complex $[S_5Fe(NO)_2]^-$ to the $[S_5Fe(\mu\text{-}S)_2FeS_5]^{2-}$ by photolysis in the presence of the NO-acceptor reagent $[(C_4H_8O)Fe(S,S{-}C_6H_4)_2]^-$ are consistent with reports of in vitro the degradation of ferredoxin [2Fe-2S] clusters to DNICs and the repair of nitric oxide-modified [2Fe−2S] ferredoxin by cysteine desulfurase and L-cysteine.[12b] In particular, the detailed spectroscopic analysis (EPR and IR $\nu_{NO}$ spectra) may provide a superior level of insight on discrimination of the anionic $\{Fe(NO)_2\}^9$ DNICs, neutral $\{Fe(NO)_2\}^9$ DNIC, and Roussin's red ester.[12a] We also demonstrated that the NO-releasing ability of the anionic $\{Fe(NO)_2\}^9$ $[(RS)_2Fe(NO)_2]^-$ is finely tuned by the coordinated thiolate ligands.[12c] The objective of this study was to delineate the formation pathway of the anionic $\{Fe(NO)_2\}^9$ DNICs $[(RS)_2Fe(NO)_2]^-$ from nitrosylation of the biomimetic oxidized- and reduced-form rubredoxin $[Fe(SR)_4]^{2-/1-}$ (R = Ph, Et)[16] and to elucidate the reactivity of the mononitrosyl tris(thiolate) complexes $[Fe(NO)(SR)_3]^-$, an intermediate for the conversion of $[Fe(SR)_4]^{2-/1-}$ into DNICs in the presence of $NO_{(g)}$. In addition, the anionic $\{Fe(NO)\}^7$ $[Fe(NO)(SPh)_3]^-$ containing monodentate phenylthiolates and the anioinic $\{Fe(NO)_2\}^9$ $[(EtS)_2Fe(NO)_2]^-$ containing monodentate ethylthiolates coordinated to the $\{Fe(NO)_2\}$ unit were isolated and characterized by X-ray diffraction.

## Results and Discussion

**Nitrosylation of $[Fe(SPh)_4]^{2-/1-}$.** Upon addition of 1 equiv of $NO_{(g)}$ into the $CH_3CN$ solution of the biomimetic reduced-form rubredoxin $[Fe^{II}(SPh)_4]^{2-}$,[16] a pronounced color change from red-brown to purple occurs at 0 °C. The IR, UV−vis, and single-crystal X-ray diffraction studies confirmed the formation of the mononitrosyl tris(phenylthiolate) complex $[Fe(NO)(SPh)_3]^-$ (**1**) (yield 78%) accompanied by byproduct


(6) Drapier, J. C. *Methods* **1997**, *11*, 319−329.
(7) Bryan, N. S.; Fernandez, B. O.; Bauer, S. M.; Garcia-Saura, M. F.; Milsom, A. B.; Rassaf, T.; Maloney, R. E.; Bharti, A.; Rodriguez, J.; Feelisch, M. *Nat. Chem. Biol.* **2005**, *1*, 290−297.
(8) Dailey, H. A.; Dailey, T. A.; Wu, C.-K.; Medlock, A. E.; Rose, J. P.; Wang, K.-F. *Cell. Mol. Life Sci.* **2000**, *57*, 1909−1926.
(9) Ding, H.; Demple, B. *Proc. Natl. Acad. Sci. U.S.A.* **2000**, *97*, 5146−5150.
(10) (a) Yang, W.; Rogers, P. A.; Ding, H. *J. Biol. Chem.* **2002**, *277*, 12868−12873. (b) Rogers, P. A.; Ding, H. *J. Biol. Chem.* **2001**, *276*, 30980−30986.
(11) (a) Chiang, C.-Y.; Miller, M. L.; Reibenspies, J. H.; Darensbourg, M. Y. *J. Am. Chem. Soc.* **2004**, *126*, 10867−10874. (b) Baltusis, L. M.; Karlin, K. D.; Rabinowitz, H. N.; Dewan, J. C.; Lippard, S. J. *Inorg. Chem.* **1980**, *19*, 2627−2632.
(12) (a) Tsai, M.-L.; Liaw, W.-F. *Inorg. Chem.* **2006**, *45*, ASAP. (b) Tsai, M.-L.; Chen, C.-C.; Hsu, I.-J.; Ke, S.-C.; Hsieh, C.-H.; Chiang, K.-A.; Lee, G.-H.; Wang, Y.; Liaw, W.-F. *Inorg. Chem.* **2004**, *43*, 5159−5167. (c) Tsai, F.-T.; Chiou, S.-J.; Tsai, M.-C.; Tsai, M.-L.; Huang, H.-W.; Chiang, M.-H.; Liaw, W.-F. *Inorg. Chem.* **2005**, *44*, 5872−5881. (d) Chen, T.-N.; Lo, F.-C.; Tsai, M.-L.; Shih, K.-N.; Chiang, M.-H.; Lee, G.-H.; Liaw, W.-F. *Inorg. Chimi. Acta* **2006**, *359*, 2525−2533. (e) Hung, M.-C.; Tsai, M.-C.; Liaw, W.-F. *Inorg. Chem.* **2006**, *45*, 6041−6047. (f) Butler, A. R.; Glidewell, C.; Li, M.-H. *Adv. Inorg. Chem.* **1988**, *32*, 335−393.
(13) Reginato, N.; McCrory, C. T. C.; Pervitsky, D.; Li, L. *J. Am. Chem. Soc.* **1999**, *121*, 10217−10218.
(14) Enemark, J. H.; Feltham, R. D.*Coord. Chem. Rev.* **1974**, *13*, 339−406.
(15) (a) Harrop, T. C.; Song, D. T.; Lippard, S. J. *J. Am. Chem. Soc.* **2006,** *128*, 3528−3529. (b) Jaworska, M.; Stasicka, Z. *J. Organomet. Chem.* **2004**, *689*, 1702−1713.
(16) (a) Rao, P. V.; Holm, R. H. *Chem. Rev.* **2004**, *104*, 527−559. (b) Arulsamy, N.; Bohle, D. S.; Butt, J. A.; Irvine, G. J.; Jordan, P. A.; Sagan, E. *J. Am. Chem. Soc.* **1999**, *121*, 7115−7123.

**Scheme 1**

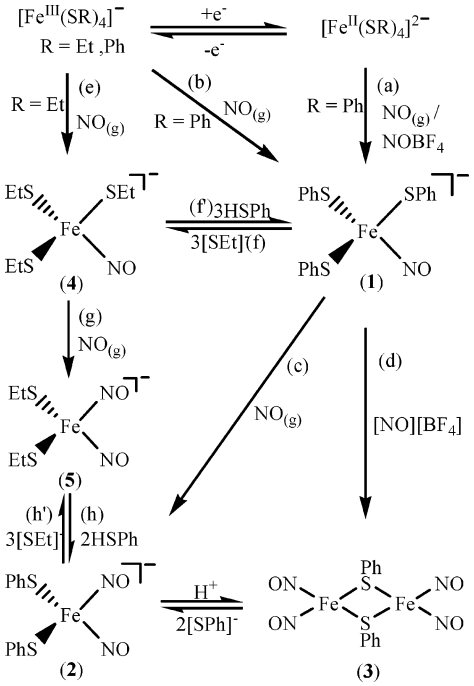


[PPN][SPh] identified by IR (KBr) and $^1$H NMR (Scheme 1a). Instead of phenylthiolate-ligand displacement observed in the reaction of $[Fe^{II}(SPh)_4]^{2-}$ and $NO_{(g)}$, reaction of $NO_{(g)}$ with the oxidized-form $[Fe^{III}(SPh)_4]^-$ in a 1:1 stoichiometry in $CH_3CN$ also led to the formation of complex **1** but accompanied by byproduct $(PhS)_2$ characterized by IR (KBr) and $^1$H NMR (Scheme 1b). Obviously, NO radical binding to an electron-deficient iron(III) center of complex $[Fe^{III}(SPh)_4]^-$ triggers reductive elimination of the coordinated phenylthiolate ligand to yield complex **1** and diphenyl disulfide, in contrast to the phenylthiolate-ligand elimination observed in the nitrosylation of complex $[Fe^{II}(SPh)_4]^{2-}$ containing the relative electron-rich iron(II) center.

Complex **1** is extremely air- and light-sensitive in solution and solid states. The EPR spectrum ($g$ values at 3.76 and 2.012 in $CH_2Cl_2$−toluene (1:1 volume ratio) frozen solution at 4 K, Supporting Information Figure S1)[12f,15] and the magnetic measurement (the temperature-dependent effective magnetic moment $\mu_{eff}$ decreases from 3.83 $\mu_B$ at 300 K to 3.66 $\mu_B$ at 50 K, Supporting Information Figure S2) of complex **1** are consistent with the Fe(III)−NO− electronic configuration in a tetrahedral ligand field, as characterized by Lippard and co-workers in complex $[Fe(NO)(S^tBu)_3]^-$.[15] The infrared spectrum of complex **1** shows one broad stretching band (1726 (KBr), 1732 cm$^{-1}$ (THF)) in the $\upsilon_{NO}$ region, which shifts to 1697 cm$^{-1}$ (THF) upon isotopic substitution with $^{15}$NO. The higher-energy $\upsilon_{NO}$ band of complex **1** shifted by 22 cm$^{-1}$ from that of complex $[Fe(NO)(S^tBu)_3]^-$ ($\nu_{NO}$ 1704 cm$^{-1}$ (KBr)) is consistent with the weaker electron-donating character of $[PhS]^-$ ligand, compared to $[S^tBu]^-$ (Table 1).[15] In addition, the formation of complex **1** was also displayed by reaction of $[Fe^{II}(SPh)_4]^{2-}$ and $[NO][BF_4]$. When a $CH_3CN$ solution of complex $[Fe^{II}(SPh)_4]^{2-}$ was treated with 1 equiv of $[NO][BF_4]$, an immediate change in color of the solution from red-brown to purple was observed. The reaction mixture led to the isolation of the extremely air- and light-sensitive complex **1**, accompanied by byproduct $(PhS)_2$ identified by IR and $^1$H NMR. Interestingly, reaction of $[Fe^{II}(SPh)_4]^{2-}$ and [PPN]-$[NO_2]$, the NO-derived molecule, also led to the formation of complex **1** in $CH_2Cl_2$.

**Table 1.** Selected Infrared and UV−vis Data for the MNICs and DNICs

| complex | IR (cm$^{-1}$) | UV (nm) | ref |
|---|---|---|---|
| MNICs | | | |
| **1** | 1731[a] | 500[a] | this work |
| **4** | 1697[a] | 459[a] | this work |
| $[Et_4N][Fe(S^tBu)_3(NO)]^-$ | 1703[a] | 370, 475[a] | 15a |
| DNICs | | | |
| **2** | 1693, 1737[a] | 479, 798[a] | this work |
| **5** | 1674, 1715[a] | 436, 802[a] | this work |
| $[PPN][(S(CH_2)_3S)Fe(NO)_2]$ | 1671, 1712[a] | 430, 578, 807[a] | 12e |
| $[Et_4N][(S^tBu)_2Fe(NO)_2]^-$ | 1690, 1739[b] | N/A | 15a |
| $(H^+bme\text{-}daco)Fe(NO)_2$ | 1696, 1740[a] | N/A | 11a |
| $[(C_9H_{21}N_2S_2)Fe(NO)_2]$ | 1695, 1740[c] | N/A | 11b |

[a] THF. [b] $CH_3CN$. [c] KBr.

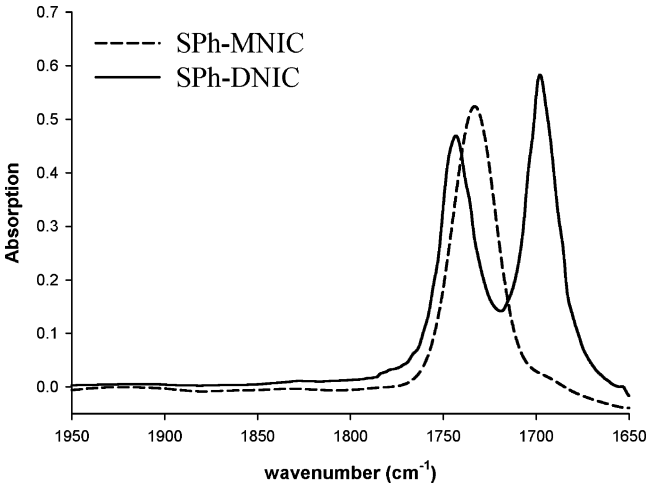


**Figure 1.** Infrared $\nu_{NO}$ absorbance changes for the reaction of complex **1** with $NO_{(g)}$ in a 1:1 stoichiometry in $CH_3CN$ at ambient temperature. Curve (− −) corresponds to complex **1**, and curve (—) corresponds to the formation of complex **2**.

When 1 equiv of $NO_{(g)}$ (or $[(Ph)_3CSNO]$) was added to the THF solution of complex **1** at ambient temperature, a rapid reaction occurred to afford the well-known dinitrosyl iron complex $[(PhS)_2Fe(NO)_2]^-$ (**2**) accompanied by the liberation of diphenyl disulfide identified by IR (KBr) and $^1$H NMR (Scheme 1c). The shift of the $\nu_{NO}$ stretching frequencies from 1734 (complex **1**) to 1745, 1698 cm$^{-1}$ ($CH_3$-CN) confirmed the formation of complex **2** (Figure 1). The conversion of complexes **1** to **2** was also monitored by UV−vis spectrometry; the intense band at 500 nm disappeared, accompanied by the simultaneous formation of two absorption bands at 479 and 798 nm (complex **2**) (Figure 2). As observed in the nitrosylation of the $[Fe^{III}(SPh)_4]^-$ complex, the reaction mechanism, NO binding to the electron-deficient iron(III) center of complex **1** triggering the reductive elimination of the coordinated phenylthiolate ligand to yield complex **2**, was proposed. Instead of the formation of complex **2**, treatment of complex **1** with 1 equiv of [NO]-$[BF_4]$ in THF solution at ambient temperature led to the

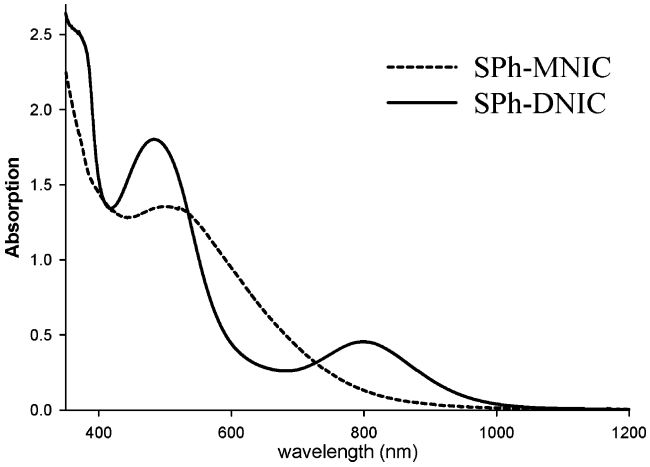


**Figure 2.** Conversion of complex **1** to complex **2** monitored by UV−vis spectrometry under addition of 1 equiv of $NO_{(g)}$ to complex **1** in THF at ambient temperature. The absorption band at 500 nm (− −) disappeared followed by the simultaneous formation of two absorption bands at 479 and 798 nm (−).

**Scheme 2**

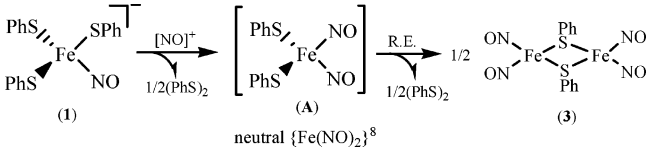


formation of $[Fe_2(\mu\text{-SPh})_2(NO)_4]$ (**3**) (yield 95%),[17] and the byproduct $(PhS)_2$ identified by IR (KBr) and $^1$H NMR. The formation of complex **3** under $[NO]^+$ oxidation of complex **1** may be accounted for by the following reaction sequence; the $[NO]^+$ oxidant has available only the ability of oxidizing the coordinated phenylthiolate of complex **1** to produce a thiyl radical ($[PhS]^\bullet$) (subsequently coupled to yield $(PhS)_2$) and NO radical, followed by the rapid binding of a generated NO radical leading to the buildup of unstable, neutral $\{Fe(NO)_2\}^8$ $[(PhS)_2Fe(NO)_2]$ (**A**) species (Scheme 2). This highly reactive, neutral $\{Fe(NO)_2\}^8$ species **A** is then driven by the formation of complex **3** via an intramolecular reductive elimination of diphenyl disulfide (Scheme 2).

**Nitrosylation of $[Fe^{III}(SEt)_4]^-$.** To further corroborate the formation mechanism of DNICs from nitrosylation of $[Fe(SR)_4]^{2-/1-}$ and investigate the stability/reactivity of the anionic $\{Fe(NO)\}^7$ MNICs $[Fe(NO)(SR)_3]^-$ and $\{Fe(NO)_2\}^9$ DNICs $[(RS)_2Fe(NO)_2]^-$, the reaction of the biomimetic oxidized-form rubredoxin $[Fe^{III}(SEt)_4]^-$ was investigated. As shown in Scheme 1e, when complex $[Fe^{III}(SEt)_4]^-$ was treated with 1 equiv of $NO_{(g)}$ in $CH_3CN$ at 0 °C, a rapid reaction ensues over the course of 1 min to give the stable, purple complex $[Fe(NO)(SEt)_3]^-$ (**4**) (yield 74%) after removal of $(SEt)_2$ identified by IR (KBr) and $^1$H NMR. In comparison with complex **1** dominated by one intense absorption band at 500 nm (THF), the electronic spectrum of complex **4** coordinated by the more electron-donating ethylthiolates displays a blue-shift to 459 nm (Table 1). In contrast to complex **1**, which is unstable in THF solution, the ligand-modified analogue complex **4** displays more stability to light. Presumably, the more electron-donating functionality of the coordinated ethylthiolates in complex **4** is responsible for the stabilization of the [Fe(III)−$NO^-$] state.[15]

Consistent with the stronger electron-donating thiolates $[R'S]^-$ promoting thiolate-ligand exchange of complex $[(RS)_2Fe(NO)_2]^-$ to produce the stable $[(R'S)_2Fe(NO)_2]^-$ observed in the previous study,[12c] quantitative transformation of complex **1** to complex **4** was displayed and monitored by IR $\nu_{NO}$ spectra. The shift of the NO stretching frequency from 1734 $cm^{-1}$ to the lower frequency 1704 $cm^{-1}$ confirmed the formation of complex **4** (yield 90%) when $CH_3CN$ solution of complex **1** was reacted with 3 equiv of $[SEt]^-$ (Scheme 1f). Complex **4** does not react with $[SPh]^-$ via thiolate-ligand exchange to form complex **1**. Conversion of complex **4** to complex **1** was expected to be driven by protonation (PhSH) of complex **4**; reaction of complex **4** and 3 equiv of thiophenol in THF led to the isolation of complex **1**. Presumably, protonation (electrophilic reaction of PhSH) of complex **4** by thiophenol occurs only at the more accessible, electron-rich sulfur site to form complex **1** (yield 95%) at ambient temperature (Scheme 1f). Obviously, mononitrosyl tris(phenylthiolate) complex **1** containing the coordinated phenylthiolate ligands and complex **4** containing the coordinated ethylthiolate ligands are chemically interconvertible.

**Isolation of the Stable $[(EtS)_2Fe(NO)_2]^-$ (5) with Ethylthiolates Coordinated to a $\{Fe(NO)_2\}^9$ Motif.** Of importance is that the conversion of complex **4** to the stable $[(EtS)_2Fe(NO)_2]^-$ (**5**) was displayed when 1 equiv of $NO_{(g)}$ was added to the THF solution of complex **4** at ambient temperature (Scheme 1g), the color of the solution changed from red to reddish-brown, where the IR $\upsilon_{NO}$ stretching frequency at 1697 $cm^{-1}$ (THF) disappeared with the formation of two stretching frequencies at 1715 and 1674 $cm^{-1}$ (THF). The dark red-brown complex **5** was isolated in 90% yield after the reaction solution was separated from $(SEt)_2$ and recrystallized with hexane. Consistent with the characteristic $g$ value of DNICs,[9−15] complex **5** exhibits an isotropic EPR spectrum with signal at $g = 2.028$ at 298 K (Supporting Information Figure S3).[12f] Magnetic susceptibility data of a powdered sample of complex **5** was collected in the temperature range of 2−300 K in a 0.5 T applied field. The effective magnetic moment ($\mu_{eff}$) decreases from 2.8 at 300 K to 1.77 at 8 K (Supporting Information Figure S4). As observed in the previous study,[12c] the temperature-dependent magnetic moment in complex **5** may be contributed from the antiferromagnetic interactions between the $Fe^+$ ($d^7$, $S = 3/2$) center and two $^\bullet NO$ ($S = 1/2$) radicals, and the dynamic resonance hybrid of $\{Fe^+(^\bullet NO)_2\}^9$ and $\{Fe^-(^+NO)_2\}^9$ by temperature. The IR spectra for DNICs **2** and **5** had the same pattern but differed in position (1737, 1693 $cm^{-1}$ for complex **2** vs 1715, 1674 $cm^{-1}$ for complex **5**). The surprisingly stable complex **5** is the first example of the anionic $\{Fe(NO)_2\}^9$ DNICs $[(RS)_2Fe(NO)_2]^-$ containing monodentate alkylthiolates coordinated to the $\{Fe(NO)_2\}^9$ motif isolated and characterized by single-crystal X-ray diffraction.[11] This complex represents an important starting point to understand

(17) Rauchfuss, T. B.; Weatherill, T. D. *Inorg. Chem.* **1982**, *21*, 827−830.

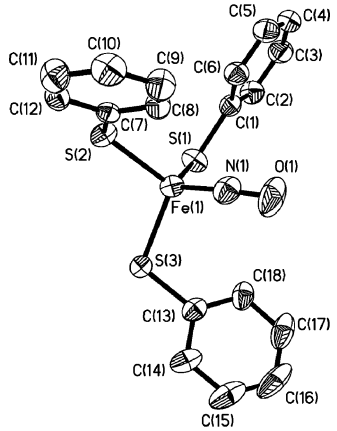


**Figure 3.** ORTEP drawing and labeling scheme of [Fe(NO)(SPh)$_3$]$^-$ with thermal ellipsoids drawn at 50% probability. Selected bond distances (Å) and angles (deg): Fe(1)−N(1) 1.682(5); Fe(1)−S(3) 2.2670(14); Fe(1)−S(1) 2.2696(12); Fe(1)−S(2) 2.2780(13); O(1)−N(1) 1.169(6); N(1)−Fe(1)−S(3) 108.69(18); N(1)−Fe(1)−S(1) 109.19(18); S(3)−Fe(1)−S(1) 103.87(5); N(1)−Fe(1)−S(2) 116.52(16); S(3)−Fe(1)−S(2) 108.35(5); S(1)−Fe(1)−S(2) 109.47(5).

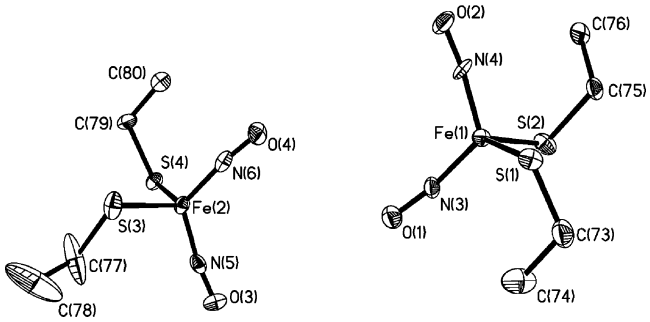


**Figure 4.** ORTEP drawing and labeling scheme of [(EtS)$_2$Fe(NO)$_2$]$^-$ with thermal ellipsoids drawn at 50% probability. Selected bond distances (Å) and angles (deg): Fe(1)−N(3) 1.673(6); Fe(1)−N(4) 1.674(6); Fe(1)−S(1) 2.2659(19); Fe(1)−S(2) 2.283(2); Fe(2)−N(5) 1.679(6); Fe(2)−N(6) 1.678(6); Fe(2)−S(3) 2.269(2); Fe(2)−S(4) 2.273(2); O(1)−N(3) 1.194(6); O(2)−N(4) 1.188(7); O(3)−N(5) 1.180(7); O(4)−N(6) 1.182(7); N(3)−Fe(1)−N(4) 121.5(3); N(3)−Fe(1)−S(1) 108.6(2); N(4)−Fe(1)−S(1) 99.8(2); N(3)−Fe(1)−S(2) 107.7(2); N(4)−Fe(1)−S(2) 111.4(2); S(1)−Fe(1)−S(2) 106.72(8); N(5)−Fe(2)−N(6) 123.1(3); N(5)−Fe(2)−S(3) 109.9(2); N(6)−Fe(2)−S(3) 107.0(2); N(5)−Fe(2)−S(4) 99.3(2); N(6)−Fe(2)−S(4) 108.66(19); S(3)−Fe(2)−S(4) 107.91(8).

the factors that are responsible for the stability and reactivity of the anionic {Fe(NO)$_2$}$^9$ alkylthiolate-containing DNICs.

Transformation of complex **5** to complex **2** was displayed when reaction of complex **5** and 2 equiv of thiophenol in THF. Consistent with the facile conversion of complex **1** to complex **4** under reaction of complex **1** and 3 equiv of [SEt]$^-$, the coordinated [SPh]$^-$ ligands of complex **2** were replaced by the stronger electron-donating ethylthiolate [SEt]$^-$ to yield complex **5** when reacting complex **2** with 3 equiv of [SEt]$^-$ (or more) in $CH_3CN$ at ambient temperature (Scheme 1h′). Conversion of complex **2** into complex **5** was observed only in the presence of 3 equiv (or more) of [SEt]$^-$ and complex **2** in $CH_3CN$ at ambient temperature.

**Structures.** Figures 3 and 4 display the thermal ellipsoid plot of the anionic complexes **1** and **5**, respectively, and selected bond distances and angles are given in the figure captions. The N(1)−Fe(1)−S(3), N(1)−Fe(1)−S(1), S(3)−Fe(1)−S(2), and S(1)−Fe(1)−S(2) bond angles of 108.69(18)°, 109.19(18)°, 108.35(5)°, and 109.47(5)°, respectively, are consistent with the distorted tetrahedral coordination environment about Fe(1) of complex **1**. It is noticed that the NO bond length of 1.169(6) Å in complex **1** is longer than that of 1.1677(19) Å in complex [Fe(NO)(S$^t$Bu)$_3$]$^-$, and the Fe(1)N(1) bond length of 1.682(5) Å in complex **1** is shorter than that of 1.7110(14) Å in complex [Fe(NO)(S$^t$Bu)$_3$]$^-$ (Table 2).[15a] Interestingly, the Fe−N−O bond angle of 164.6(5)° in complex **1** is distinct from that of 174.18(13)° in complex [Fe(NO)(S$^t$Bu)$_3$]$^-$.[15a] The changes in Fe−N−O bond angle from the bent form (164.6(5)° for complex **1**) to the less-bent form (170.3(6)°/172.9(6)° for complex **5**) are, presumably, caused by electronic perturbation from the {Fe(NO)}$^7$ complex **1** to the {Fe(NO)$_2$}$^9$ complex **5**. The X-ray crystal structure of complex **5** consists of two crystallographically independent molecules (Figure 4). The geometry of iron center of complex **5** is best described as a distorted tetrahedral with N(3)−Fe(1)−N(4), N(4)−Fe(1)−S(1), and S(1)−Fe(1)−S(2) bond angles of 121.5(3)°, 99.8(2)°, and 106.72(8)°, respectively. The mean NO bond distances of 1.191(7) (1.194(6) and 1.188(7) Å) and 1.181(7) Å (1.180(7) and 1.182(7) Å) in complex **5**, comparable to the average NO bond distance of 1.186(7) Å observed in [(H$^+$bme-daco)Fe(NO)$_2$] (Table 3),[11a] are nearly at the upper end of the 1.178(3)−1.160(6) Å for the anionic {Fe(NO)$_2$}$^9$ DNICs, while the mean FeN(O) distances of 1.674(6) Å (or 1.679(6) Å) in complex **5** exactly fall in the range of 1.695(3)−1.661(4) Å for the anionic {Fe(NO)$_2$}$^9$ DNICs.[12]

**Table 2.** Selected Bond Length (Å) and Angle (deg) for Complex **1** and [Fe(S$^t$Bu)$_3$((NO)]$^-$ [15a]

| complex | **1** | [Fe(S$^t$Bu)$_3$(NO)]$^-$ |
|---|---|---|
| Fe−N | 1.682 | 1.171 |
| Fe−S (average) | 2.272 | 2.274 |
| N−O | 1.169 | 1.168 |
| N−Fe−S | 108.7 | 103.2 |
| N−Fe−S | 109.2 | 109.2 |
| N−Fe−S | 116.5 | 113.2 |
| S−Fe−S | 103.9 | 105.4 |
| S−Fe−S | 108.4 | 109.9 |
| S−Fe−S | 109.5 | 116.1 |
| Fe−N−O | 164.6 | 174.2 |

**Conclusion and Comments.** Studies on nitrosylation of the biomimetic reduced- and oxidized-form rubredoxin [Fe(SR)$_4$]$^{2-/1-}$ (R = Ph, Et) and the reactivity/transformation between mononitrosyl tris(thiolate) iron complexes [Fe(NO)(SR)$_3$]$^-$ and dinitrosyl iron complexes [(RS)$_2$Fe(NO)$_2$]$^-$ have resulted in the following results.

(1) Nitrosylation of complexes [Fe(SR)$_4$]$^{2-/1-}$ (R = Ph, Et) in a 1:1 stoichiometry led to the formation of the extremely air- and light-sensitive mononitrosyl tris(thiolate) iron complexes [Fe(NO)(SR)$_3$]$^-$ along with byproducts [SR]$^-$ or (RS)$_2$. The facile transformations of MNICs [Fe(NO)(SR)$_3$]$^-$ into DNICs [(RS)$_2$Fe(NO)$_2$]$^-$ and [Fe$_2$($\mu$-SR)$_2$(NO)$_4$] under 1 equiv of NO$_{(g)}$ and [NO]$^+$, respectively, were also demonstrated. Obviously, the mononitrosyl tris(thiolate) complex [Fe(NO)(SR)$_3$]$^-$ serves as an intermediate during the nitrosylation of the biomimetic oxidized- and reduced-form rubredoxin [Fe(SR)$_4$]$^{2-/1-}$ to form [(RS)$_2$Fe(NO)$_2$]$^-$.

(2) Reductive elimination of dialkyl/diphenyl disulfides occurs when NO binds to the electron-deficient Fe(III) [Fe$^{III}$-

**Table 3.** Selected Bond Lengths (Å) and Angles (deg) for Complex **5**, $[(C_9H_{21}N_2S_2)Fe(NO)_2]$,[11b] $[(H^+Bme\text{-}daco)Fe(NO)_2]$,[11a] and $[(S(CH_2)_3S)Fe(NO)_2]^-$ [12e]

| complex | **5** | $(C_9H_{21}N_2S_2)Fe(NO)_2$ | $(H^+bme\text{-}daco)Fe(NO)_2$ | $[(S(CH_2)_3S)Fe(NO)_2]^-$ |
|---|---|---|---|---|
| Fe−N | 1.676 | 1.680 | 1.669 | 1.676 |
| Fe−S | 2.273 | 2.270 | 2.278 | 2.258 |
| N−O | 1.186 | 1.160 | 1.186 | 1.178 |
| N−Fe−N | 122.3 | 118.1 | 117.5 | 118.6 |
| N−Fe−S | 99.6 | 103.5 | 103.4 | 107.6 |
| N−Fe−S | 107.8 | 103.8 | 103.6 | 107.9 |
| N−Fe−S | 108.6 | 111.5 | 110.0 | 108.5 |
| N−Fe−S | 110.7 | 118.8 | 111.7 | 111.7 |
| S−Fe−S | 106.9 | 109.2 | 111.1 | 100.9 |
| Fe−N−O | 172.1 | 169.8 | 171.5 | 170.1 |

**Scheme 3**

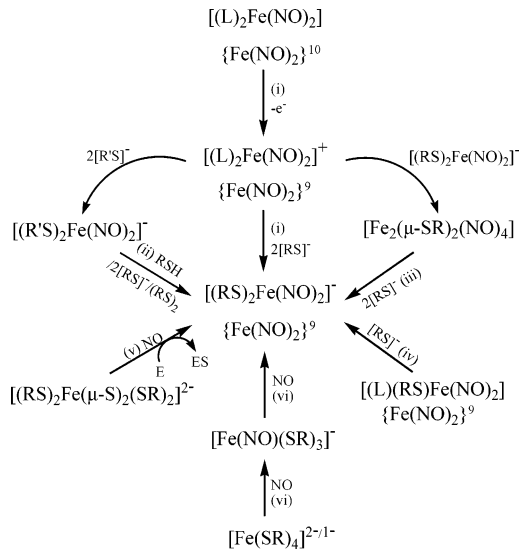


$(SR)_4]^-$/$[Fe^{III}(NO)(SR)_3]^-$ complexes, while binding of NO radical to the reduced-form $[Fe^{II}(SR)_4]^{2-}$ induces the thiolate-ligand ($[SR]^-$) elimination.

(3) Complex **1** containing phenylthiolates coordinated to $\{Fe(NO)\}^7$ motif and complex **5** containing ethylthiolates coordinated to $\{Fe(NO_2)\}^9$ motif were isolated and characterized by X-ray diffraction. The mean Fe−N(O) distances of 1.674(6) Å (or 1.679(6) Å) in complex **5** exactly fall in the range of 1.695(3)−1.661(4) Å for the anionic $\{Fe(NO_2)\}^9$ DNICs.[12e]

(4) In addition to the combination reaction of iron salts, NO and ligands $[RS]^-$ yielding a EPR-detectable, four-coordinated DNICs,[18] six synthetic routes leading to the formation of the anionic $\{Fe(NO_2)\}^9$ $[(RS)_2Fe(NO)_2]^-$ were demonstrated (Scheme 3): (i) the facile transformation of the neutral $\{Fe(NO_2)\}^{10}$ $[(L)_2Fe(NO)_2]$ (L = N-containing neutral ligands) to the anionic $\{Fe(NO_2)\}^9$ $[(RS)_2Fe(NO)_2]^-$ via the cationic $\{Fe(NO_2)\}^9$ $[(L)_2Fe(NO)_2]^+$ followed by addition of 2 equiv of thiolates,[12e] (ii) reaction of the anionic $\{Fe(NO_2)\}^9$ $[(R'S)_2Fe(NO)_2]^-$ and PhSH/$[RS]^-$/$(RS)_2$ yielding the stable anionic $\{Fe(NO_2)\}^9$ $[(RS)_2Fe(NO)_2]^-$ by protonation, ligand-exchange reaction and S−S bond activation, respectively,[12] (iii) conversion of Roussin's red ester into the anionic $[(RS)_2Fe(NO)_2]^-$ triggered by the nucleophilic thiolates inducing the cleavage of bridging thiolates,[12] (iv) transformation of the neutral $\{Fe(NO_2)\}^9$ $[(RS)(L')Fe(NO)_2]$ (L′ = N-containing ligand) to the anionic $\{Fe(NO_2)\}^9$ $[(RS)_2Fe(NO)_2]^-$ by ligand replacement,[12a] (v) the direct nitrosylation of the biomimetic [2Fe-2S] cluster in the presence of S-trapping agent,[12b] and (vi) the direct nitrosylation of the biomimetic reduced- and oxidized-form rubredoxin $[Fe(SR)_4]^{2-/1-}$ via intermediate MNIC $[Fe(NO)(SR)_3]^-$,[15a] as shown in this study (Scheme 3).

These results may also predict/decipher that the most straightforward and facile pathway of the formation of the anionic $\{Fe(NO_2)\}^9$ DNICs $[(RS)_2Fe(NO)_2]^-$ is the direct nitrosylation of $[Fe_m(SR)_n]^{x-}$ clusters (e.g., $[Fe(SR)_4]^{2-/1-}$ and $[(RS)_2Fe(\mu\text{-}S)_2Fe(SR)_2]^{2-}$), i.e., the direct nitrosylation of [1Fe-0S]/[2Fe-2S] iron−sulfur proteins in biology. Presumably, the formation of DNICs via combination of $Fe^{2+}$ ion, *S*-cysteine and NO, as suggested by biochemists,[1−2,18] may occur through the original formation of the $[Fe_m(SR)_n]^{x-}$ clusters followed by nitrosylation as observed in this study.

For the synthetic methodology, the isolation of complex **5** shows that the synthetic pathway may play a key role in synthesizing the stable DNICs $[(RS)_2Fe(NO)_2]^-$ containing alkylthiolates coordinated to $\{Fe(NO_2)\}^9$ motif.[11,12]

## Experimental Section

Manipulations, reactions, and transfers were conducted under nitrogen according to Schlenk techniques or in a glovebox (argon gas). Solvents were distilled under nitrogen from appropriate drying agents (diethyl ether from $CaH_2$; acetonitrile from $CaH_2/P_2O_5$; methylene chloride from $CaH_2$; methanol from $Mg/I_2$; hexane and tetrahydrofuran (THF) from sodium benzophenone) and stored in dried, $N_2$-filled flasks over 4 Å molecular sieves. Nitrogen was purged through these solvents before use. Solvent was transferred to the reaction vessel via stainless cannula under positive pressure of $N_2$. The reagents thiophenol, sodium nitrite, nitrosonium tetrafluroborate ($[NO][BF_4]$), iron trichloride, ethanethiol (Aldrich), bis(triphenylphosphoranylidene)ammonium chloride ([PPN][Cl]) (Fluka) were used as received. The $NO_{(g)}$ (SanFu, 10% NO + 90% $N_2$) was passed through an Ascarite II column to remove higher nitrogen oxides before use.[19] Compounds $[PPN]_2[Fe^{II}(SPh)_4]$,[16a] $[PPN][Fe^{III}(SPh)_4]$,[16a] $[PPN][Fe^{III}(SEt)_4]$,[16a] and *S*-nitrosothiol ($[(Ph)_3CSNO]$)[16b] were synthesized by published procedures. Infrared spectra of the $\nu_{NO}$ stretching frequencies were recorded on a PerkinElmer model spectrum One B spectrometer with sealed solution cells (0.1 mm, KBr windows). UV−vis spectra were

(18) McDonald, C. C.; Phillips, W.; Mower, H. F. *J. Am. Chem. Soc.* **1965**, *87*, 3319−3326.

(19) Works, C. F.; Jocher, C. J.; Bart, G. D.; Bu, X.; Ford, P. C. *Inorg. Chem.* **2002**, *41*, 3728−3739.

recorded on a Jasco V-570 spectrometer. Analyses of carbon, hydrogen, and nitrogen were obtained with a CHN analyzer (Heraeus).

**Reaction of [PPN]$_2$[Fe$^{II}$(SPh)$_4$] and NO$_{(g)}$. Method A.** Under $N_2$ atmosphere, to a $CH_3CN$ solution (3 mL) of [PPN]$_2$[Fe(SPh)$_4$] (0.16 g, 0.1 mmol) was added $NO_{(g)}$ (24 mL (10% NO + 90% $N_2$), 0.1 mmol) via a gastight syringe at 0 °C. The reaction solution was stirred and monitored by FTIR immediately. The IR $\upsilon_{NO}$ spectrum shows a strong stretching band at 1734 cm$^{-1}$ ($CH_3CN$). The solution was then dried under vacuum, and the crude solid was redissolved in THF/diethyl ether (1:1 volume ratio). The mixture solution was filtered to remove the insoluble [PPN][SPh] characterized by IR (KBr) and $^1$H NMR. Addition of hexane to the filtrate (THF/diethyl ether solution) led to the precipitation of dark purple solid [PPN][Fe(SPh)$_3$(NO)] (**1**) (yield 0.74 g, 78%). Hexane was added slowly to the layer above the THF solution of complex **1**. The flask was tightly sealed and kept in the refrigerator at 10 °C for 4 days. The dark purple crystals suitable for X-ray diffraction analysis were isolated.

**Method B.** A $CH_3CN$ solution (7 mL) of [NO][$BF_4$] (0.058 g, 0.5 mmol) was added in a dropwise manner to a $CH_3CN$ solution of [PPN]$_2$[Fe(SPh)$_4$] (0.79 g, 0.5 mmol) at 0 °C under $N_2$ atmosphere. The reaction solution was stirred for 10 min. The IR $\nu_{NO}$ spectrum shows a strong absorption band at 1734 cm$^{-1}$. The solution mixture was then dried under vacuum. The crude solid was redissolved in THF and then filtered to remove the insoluble [PPN][$BF_4$]. Hexane was then added to precipitate the dark purple solid [PPN][Fe(SPh)$_3$(NO)] (**1**) (yield 0.4 g, 84%), and the byproduct $(PhS)_2$ soluble in THF/hexane solution was isolated and identified by IR (KBr) and $^1$H NMR.

**Method C (Reaction of [PPN]$_2$[Fe$^{II}$(SPh)$_4$] and [PPN][$NO_2$]).** Complexes [PPN]$_2$[Fe(SPh)$_4$] (0.314 g, 0.2 mmol) and [PPN][$NO_2$] (0.117 g, 0.2 mmol) loaded in a 10-mL tube were dissolved in $CH_2Cl_2$ (7 mL). The solution was stirred for 10 min at ambient temperature under $N_2$ atmosphere. The IR $\nu_{NO}$ spectrum shows a strong absorption band at 1737 cm$^{-1}$. Hexane was added to precipitate the dark purple solid, and the dark purple solid was dried after solvent was removed. The crude solid was then redissolved in THF. The mixture solution was filtered to remove the insoluble solid, and hexane was added to lead to the precipitation of [PPN][Fe(SPh)$_3$(NO)] (**1**) (yield 0.076 g, 40%). IR $\nu_{NO}$: 1732 (THF), 1734 ($CH_3CN$), 1737 cm$^{-1}$ ($CH_2Cl_2$). IR $\nu^{15}{}_{NO}$: 1697 cm$^{-1}$ (THF). Absorption spectrum (THF) [$\lambda_{max}$, nm ($\epsilon$, M$^{-1}$ cm$^{-1}$)]: 500 (1951). Anal. Calcd for $C_{54}H_{45}N_2OP_2S_3Fe$: C, 68.13; H, 4.76; N, 2.94. Found: C, 68.65; H, 5.18; N, 2.92.

**Reaction of [PPN][Fe$^{III}$(SPh)$_4$] and NO$_{(g)}$.** To a $CH_3CN$ solution (5 mL) of [PPN][Fe(SPh)$_4$] (0.21 g, 0.2 mmol) was added $NO_{(g)}$ (48 mL (10% NO + 90% $N_2$), 0.2 mmol) via a gastight syringe at 0 °C, followed by stirring another 5 min at ambient temperature under $N_2$ atmosphere. The IR $\nu_{NO}$ spectrum shows a strong absorption band at 1734 cm$^{-1}$ ($CH_3CN$) assigned to the formation of complex **1**. Solvent was then removed under vacuum. The crude solid was redissolved in THF and recrystallized in THF/hexane. The byproduct $(PhS)_2$ soluble in THF/hexane solution was then isolated and identified by IR and $^1$H NMR. The dark purple crystals were collected, washed with diethyl ether, and dried to afford complex **1** (yield 0.064 g, 34%) characterized by IR and UV−vis.

**Reaction of [PPN][Fe(SPh)$_3$(NO)] (1) and NO$_{(g)}$.** To a THF solution (3 mL) of complex **1** (0.095 g, 0.1 mmol) was added $NO_{(g)}$ (24 mL (10% NO + 90% $N_2$), 0.1 mmol) via a gastight syringe. The solution was stirred under anaerobic condition for 10 min at ambient temperature. The IR $\nu_{NO}$ spectrum shows two strong stretching bands at 1737 and 1693 cm$^{-1}$ (THF), assigned to the formation of the known [PPN][$(PhS)_2$Fe(NO)$_2$] (**2**).[12c] Hexane was added to precipitate complex **2** (yield 0.063 g, 72%) characterized by IR ($\nu_{NO}$ 1737, 1693 cm$^{-1}$ (THF)) and UV−vis (479, 798 nm (THF)), and byproduct $(PhS)_2$ soluble in THF/hexane solution was isolated and identified by IR (KBr) and $^1$H NMR.

**Reaction of [PPN][Fe(SPh)$_3$(NO)] (1) and [NO][$BF_4$].** A $CH_3CN$ solution (7 mL) of [NO][$BF_4$] (0.058 g, 0.5 mmol) was added drop by drop to a $CH_3CN$ solution (5 mL) of complex **1** (0.476 g, 0.5 mmol) via cannula under positive $N_2$ pressure. The solution was stirred for 10 min at ambient temperature. The IR $\nu_{NO}$ spectrum displays three stretching bands at 1757 s, 1784 s, 1815 w cm$^{-1}$ ($CH_3CN$) assigned to the formation of the known [Fe$_2$($\mu$-SPh)$_2$(NO)$_4$] (**3**).[17] The solution mixture was dried under vacuum and then redissolved in THF (10 mL). The solution mixture was filtered to remove the insoluble [PPN][$BF_4$]. The filtrate was concentrated under vacuum, and then hexane was added to precipitate the red-brown complex **3** (yield 0.214 g, 95%). The byproduct $(PhS)_2$ existing in the THF/hexane solution was then isolated and identified by IR (KBr) and $^1$H NMR.

**Preparation of [PPN][Fe(SEt)$_3$(NO)] (4).** Complex [PPN][Fe(SEt)$_3$(NO)] (**4**) was prepared in the same manner as described in the synthesis of complex **1**. To a $CH_3CN$ solution (3 mL) of [PPN][Fe$^{III}$(SEt)$_4$] (0.168 g, 0.2 mmol) was added $NO_{(g)}$ (48 mL (10% NO + 90% $N_2$), 0.2 mmol) via a gastight syringe at 0 °C. The solution was stirred under anaerobic condition at room temperature for 10 min and monitored by IR. The IR $\nu_{NO}$ spectrum shows a strong absorption at 1704 cm$^{-1}$ ($CH_3CN$). The solution was dried under vacuum, and the crude solid was redissolved in THF. Hexane was then added to precipitate complex **4** (yield 0.12 g, 74%). IR $\nu_{NO}$: 1697 cm$^{-1}$ (THF), 1704 cm$^{-1}$ ($CH_3CN$). Absorption spectrum (THF) [$\lambda_{max}$, nm ($\epsilon$, M$^{-1}$ cm$^{-1}$)]: 459(2733).

**Transformation of [PPN][Fe(SPh)$_3$(NO)] (1) into [PPN][Fe(SEt)$_3$(NO)] (4).** Complexes **1** (0.095 g, 0.1 mmol) and [PPN][SEt] (0.18 g, 0.3 mmol) were dissolved in THF (5 mL) under $N_2$ atmosphere. The solution mixture was stirred for 10 min at ambient temperature. IR $\nu_{NO}$ spectrum displaying a strong stretching band at 1697 cm$^{-1}$ (THF) shows the formation of complex **4**. Diethyl ether (5 mL) was added to the mixture solution, and then the mixture solution was filtered to remove the insoluble [PPN][SPh]. Hexane was added to the filtrate to precipitate the red-brown complex **4** (yield 0.073 g, 90%) characterized by IR and UV−vis.

**Conversion of [PPN][Fe(SEt)$_3$(NO)] (4) into [PPN][Fe(SPh)$_3$(NO)] (1).** A THF solution (3 mL) of [PPN][Fe(SEt)$_3$(NO)] (0.081 g, 0.1 mmol) was added to thiophenol (HSPh, 31 $\mu$L) by microsyringe under $N_2$ atmosphere. The reaction solution was stirred for 10 min at ambient temperature. The IR $\nu_{NO}$ spectrum showing a strong stretching band at 1732 cm$^{-1}$ shifted from 1697 cm$^{-1}$ (THF) confirmed the formation of complex **1**. Hexane was then added to precipitate the dark purple complex **1** (yield 0.09 g, 95%) characterized by IR and UV−vis.

**Reaction of [PPN][Fe(SEt)$_3$(NO)] (4) and NO$_{(g)}$.** To a THF solution (3 mL) of complex **4** (0.081 g, 0.1 mmol) was added $NO_{(g)}$ (24 mL (10% NO + 90% $N_2$), 0.1 mmol) via a gastight syringe at 0 °C. The reaction solution was stirred for 10 min at ambient temperature and monitored by IR. The IR $\nu_{NO}$ spectrum displays two bands at 1715 and 1674 cm$^{-1}$ (THF). Hexane was slowly added to precipitate the red-brown solid characterized as **5** (yield 0.054 g, 69%). Hexane was added slowly to layer above the THF solution of complex **5**. The flask was tightly sealed and kept in the refrigerator at 10 °C for 4 days. Dark red-brown crystals suitable for X-ray diffraction analysis were obtained. IR $\nu_{NO}$: 1715, 1674 cm$^{-1}$ (THF), 1722, 1680 cm$^{-1}$ ($CH_3CN$). Absorption spectrum (THF) [$\lambda_{max}$, nm ($\epsilon$, M$^{-1}$ cm$^{-1}$)]: 436(2839), 802(430). Anal. Calcd

for $C_{40}H_{40}N_3O_2P_2S_2Fe$: C, 61.86; H, 5.19; N, 5.41. Found: C, 62.57; H, 5.29; N, 5.13.

**Transformation of [PPN][(SPh)$_2$Fe(NO)$_2$] (2) into [PPN][(SEt)$_2$Fe(NO)$_2$] (5).** Complexes **2** (0.087 g, 0.1 mmol) and [PPN][SEt] (0.18 g, 0.3 mmol) were dissolved in $CH_3CN$ (5 mL) under $N_2$ atmosphere. The solution mixture was stirred for 10 min at ambient temperature. The IR $\nu_{NO}$ spectrum displaying two strong stretching bands at 1722 and 1680 cm$^{-1}$ ($CH_3CN$) shows the formation of complex **5**. Diethyl ether (5 mL) was added to the mixture solution, and then the mixture solution was filtered to remove the insoluble [PPN][SPh] and the excess [PPN][SEt]. Hexane was added to the filtrate to precipitate the red-brown complex **5** (yield 0.066 g, 90%) characterized by IR and UV−vis.

**Reaction of [PPN][Fe(SPh)$_3$(NO)] (1) and *S*-Nitrosothiol ([(Ph)$_3$CSNO]).** A $CH_2Cl_2$ solution (3 mL) of [(Ph)$_3$CSNO] (0.031 g, 0.1 mmol) was added to a $CH_2Cl_2$ (3 mL) solution of complex **1** (0.095 g, 0.1 mmol) via cannula under positive $N_2$ pressure. The reaction solution was stirred for 2 h at ambient temperature and monitored by FTIR. The IR $\nu_{NO}$ spectrum shows two strong stretching bands at 1737 and 1693 cm$^{-1}$ assigned to the formation of the known complex **2**. Addition of hexane led to precipitation of complex **2** (yield 0.077 g, 93%) characterized by IR and UV−vis.

**EPR Measurements.** EPR measurements were performed at X-band using a Bruker EMX spectrometer equipped with a Bruker TE102 cavity. The microwave frequency was measured with a Hewlett-Packard 5246L electronic counter. X-band EPR spectra of complex **1** frozen in $CH_2Cl_2$/tolune were obtained with a microwave power of 1.006 mW, frequency at 9.631 GHz, and modulation amplitude of 2.0 G at 100 kHz, and spectra of complex **5** in THF were obtained with a microwave power of 19.971 mW, frequency at 9.604 GHz, and modulation amplitude of 1.6 G at 100 kHz.

**Magnetic Measurements.** The magnetic data were recorded on a SQUID magnetometer (MPMS5 Quantum Design Company) under 0.5 (or 1) T external magnetic field in the temperature range of 2−300 K. The magnetic susceptibility data was corrected with temperature independent paramagnetism (TIP, $2 \times 10^{-4}$ cm$^3$ mol$^{-1}$) and ligands' diamagnetism by the tabulated Pascal's constants.

**Crystallography.** Crystallographic data and structure refinements parameters of complexes **1** and **5** are summarized in the Supporting Information. The crystals chosen for X-ray diffraction studies measured $0.32 \times 0.21 \times 0.20$ mm$^3$ for complex **1**, and $0.45 \times 0.35 \times 0.15$ mm$^3$ for complex **5**, respectively. Each crystal was mounted on a glass fiber and quickly coated in epoxy resin. Unit-cell parameters were obtained by least-squares refinement. Diffraction measurements for complexes **1** and **5** were carried out on a SMART Apex CCD diffractometer with graphite-monochromated Mo $K_\alpha$ radiation ($\lambda = 0.7107$ Å) and between 1.41° and 27.50° for complex **1**, between 1.42° and 27.50° for complex **5**. Least-squares refinement of the positional and anisotropic thermal parameters of all non-hydrogen atoms and fixed hydrogen atoms was based on $F^2$. A SADABS[20] absorption correction was made. The SHELXTL[21] structure refinement program was employed.

**Acknowledgment.** We gratefully acknowledge financial support from the National Science Council of Taiwan. Authors thank Miss Chun-Yu Chen (Department of Chemistry, National Tsing Hua University) for single-crystal X-ray structure determinations.

**Supporting Information Available:** X-ray crystallographic files in CIF format for the structure determinations of [PPN][Fe(NO)(SPh)$_3$] and [PPN][(EtS)$_2$Fe(NO)$_2$]. This material is available free of charge via the Internet at http://pubs.acs.org.

IC061439G

(20) Sheldrick, G. M. *SADABS, Siemens Area Detector Absorption Correction Program*; University of Göttingen: Göttingen, Germany, 1996.
(21) Sheldrick, G. M. *SHELXTL, Program for Crystal Structure Determination*; Siemens Analytical X-ray Instruments Inc.: Madison, WI, 1994.